JACS
JOURNAL OF THE AMERICAN CHEMICAL SOCIETY
pubs.acs.org/JACS
Communication

Specific Interactions between HIV-1 Env Cytoplasmic Tail and Gag Matrix Domain Probed by NMR

Manish Chaubey,[#] Hailong Gao,[#] Christy L. Lavine, Michael S. Seaman, Bing Chen,[*] and James J. Chou[*]

Cite This: https://doi.org/10.1021/jacs.5c04597
Read Online
ACCESS | Metrics & More | Article Recommendations | Supporting Information

ABSTRACT: HIV-1 envelope glycoprotein (Env) is a transmembrane protein that mediates membrane fusion during viral entry. Incorporation of a sufficient number of Envs during viral assembly is critical for viral infectivity. It has long been suggested that the interaction between Env and the matrix domain (MA) of the Gag polyprotein plays an important role in recruiting Envs to the site of viral assembly on the plasma membrane, but direct biochemical and structural evidence is lacking for such an interaction in the context of a membrane-like environment. Here, we report specific structural contacts between the cytoplasmic tail (CT) of the trimeric HIV-1 Env in bicelles and the trimeric MA. Using a combination of measurements of NMR chemical shift perturbation, intermolecular paramagnetic relaxation enhancements, and microscale thermophoresis, we found that, in DMPC-DHPC bicelles that mimic a lipid bilayer, the trimeric baseplate formed by the CT specifically interacted with the trimeric MA via mostly electrostatic interactions involving acidic residues of the CT and positively charged patches of the MA. Nonconservative substitution of these previously unrecognized acidic residues in Env resulted in drastically reduced viral infectivity. Our findings, together with early genetic and biochemical studies, indicate that specific interactions between the CT of Env and MA play a structural role during HIV-1 assembly.

The HIV-1 envelope glycoprotein (Env) fuses viral and cell membranes to allow entry of the virus into host cells to initiate infection. The Env protein is produced as a precursor, gp160, which trimerizes to $(gp160)_3$ and then undergoes cleavage by a host furin-like protease into two noncovalently associated fragments $(gp120/gp41)_3$: gp120 for receptor binding and gp41 for membrane fusion.[1−3] The full-length Env contains a heavily glycosylated ectodomain, a single-pass transmembrane domain (TMD), and a long (∼150 residues) cytoplasmic tail (CT). The three regions can all trimerize in the context of lipid bilayer,[4−9] and they are conformationally coupled.[10,11]

A plethora of structural information have been obtained for Env-receptor recognition[12−14] and Env prefusion assembly.[4,7−9,15,16] The structural basis of the controlled incorporation of Env into newly assembled virions, however, remains poorly understood. HIV-1 particle assembly is primarily driven by the Gag protein, which selectively binds to the plasma membrane (PM) via the N-terminal matrix (MA) domain. The MA is constitutively a trimer;[17,18] it contains a PI(4,5)P2 binding site that allows for preferential targeting of the Gag protein to the PM.[19,20] Although Gag by itself is capable of assembling virus-like particles,[21] the assembly of infectious virus requires incorporation of the sufficient number of Env, on average 14, in HIV-1 particles.[22]

Env is initially synthesized and inserted into the endoplasmic reticulum (ER) membrane,[23] and then trafficked to the PM via the Golgi apparatus. On the PM, the Env trimers need to colocalize with Gags to ensure its efficient incorporation into the PM region that buds out to become a new virus. One mechanism of colocalization is cotargeting of Gag and Env to the common lipid raft sites on the PM,[24−26] thereby increasing the concentration of Env packaged into viral particles. Another mechanism involves specific protein−protein interactions between Env and Gag. For example, a single L13E mutation in MA effectively blocked incorporation of Env into HIV-1 virions and such a defect could be reverted with partial deletions of the CT;[27,28] conversely, a small deletion near the C terminus of the CT reduced viral infectivity but the effect could also be reverted with single amino acid changes in the MA.[29] In addition to genetic studies, a few biochemical studies suggested interaction between the CT and MA for SIV and HIV, though performed in the absence of membrane.[30−32]

Previous NMR analysis of a gp41 fragment comprising the TMD and the CT (TMD-CT) showed that the long CT, essential for efficient Env incorporation into virions for the majority of T cell lines,[33] formed a trimeric baseplate structure residing in the headgroup region of lipid bilayer,[7] suggesting the possibility of specific interaction with the trimeric MA. Indeed, cryo-electron tomography (ET) studies of immature HIV-1 virus particles revealed that trimerization of each monomer of the Gag dimer propagates the growth of the hexameric lattice[34] and suggested that the Env trimers can position distinctly on the underlying Gag hexameric lattice.[35]

Received: March 17, 2025
Revised: May 7, 2025
Accepted: May 8, 2025

Despite the multiple lines of indirect evidence from genetics and cryo-ET studies suggesting specific Env-MA interaction, direct biochemical and structural information is lacking due to the difficulties of investigating protein−protein interaction in the context of membrane mimetics. In this study, we used the bicelle-reconstituted gp41 TMD-CT trimer to investigate specific interaction with the trimeric MA. NMR measurements of the system mapped regions of the CT baseplate that interact with the MA and these regions were shown by functional mutagenesis to be critical for the assembly of infectious viruses. Our finding provides a structural explanation for the specific enrichment of Env to the virus budding sites.

To examine the direct interaction between the gp41 CT and MA by NMR, we used a gp41 fragment encompassing the TMD and CT from a clade D HIV-1 isolate 92UG024.2. Previous structural study of the gp41 TMD-CT indicated that TMD trimerization is important for the proper formation of the CT baseplate structure[7] that is presumably important for MA binding. The TMD-CT included residues 677−725 and 737−856. On the MA side, the p17 (PDB ID: 1HIW) MA construct from clade D was chosen for consistency, and it encompasses residues 1−132.

We first performed NMR chemical shift titration using the above protein constructs to test whether the proposed interaction is mediated by specific regions of the TMD-CT. Since the 2D $^{1}H-^{15}N$ correlation spectrum of the TMD-CT showed severe resonance overlap (Figure S1a), we had to use triple-resonance experiment to resolve the peaks in a third dimension ($^{13}C'$). In this experiment, (^{15}N, ^{13}C, ^{2}H)-labeled TMD-CT was reconstituted in DMPC-DH_6PC bicelles with $q \approx 0.5$ in a physiological buffer, yielding a final TMD-CT concentration of 300 μM. The NMR sample was split into three parts, which were diluted 2-fold with the same bicelle solution containing 0, 300, and 600 μM MA, resulting in TMD-CT:MA ratios of 1:0, 1:1, and 1:2, respectively. A 3D TROSY-enhanced HNCO spectrum was recorded for each of the three samples at 800 MHz ^{1}H frequency and 308 K. The chemical shift perturbations (CSPs) are categorized as strong, medium, and weak as shown in Figure 1a (perturbation of several well-resolved peaks in 2D TROSY-HSQC are shown in Figure S1b). Mapping of CSP values to the structure indicates strong perturbations clustered mainly to two regions of the CT and no effects on the TMD (Figure 1b). Specifically, the LLP3 and LLP1 regions covering the outer ring of the CT baseplate showed strong CSP (Figure S1c), suggesting that the TMD-CT and MA interaction is conformationally specific.

We next examined the interaction between TMD-CT and MA using a different molecular interaction measurement compatible with low protein concentrations. We used microscale thermophoresis (MST) that does not require protein immobilization. The TMD-CT in DMPC-DH_6PC bicelles was used as the ligand and titrated against a fixed concentration (2 nM) of DYE-tris-NTA labeled MA, which provided the dominant fluorescent signal for measuring heat induced molecular transport. A total of 16 dilutions of TMD-CT were prepared by diluting a starting solution of 300 μM TMD-CT with the same empty bicelle solution, such that the only variable among the 16 MST samples was the TMD-CT concentration. The overall MST signal vs TMD-CT concentration exhibited a clear dose−response relation that yields a dissociation constant (K_d) 24.4 ± 5.7 μM (Figure S2).

To obtain more direct structural evidence of the Env-MA interaction, we measured paramagnetic relaxation enhancement (PRE) of the TMD-CT caused by spin-labeled MA. For this experiment, the MA was labeled with MTSL (S-(1-oxyl-2,2,5,5-tetramethyl-2,5-dihydro-1*H*-pyrrol-3-yl) methylmethanesulfonothioate) at residue position 38 with the mutation S38C. We have tested several other sites for MTSL labeling, including V7C, S9C, S48C, S77C, D96C, and S111C, but these mutations led to aggregation problems on MTSL addition, suggesting that the trimeric MA complex structure is delicate and sensitive to single mutations. As in CSP measurement above, PREs were measured using (^{15}N, ^{13}C, ^{2}H)-labeled TMD-CT in DMPC-DH_6PC bicelles mixed with MTSL-labeled MA in a 1:1 ratio. Peak intensities before (I_{ox}) and after (I_{red}) reducing MTSL with ascorbic acid were measured using the 3D TROSY-enhanced HNCO experiment, and intermolecular PREs were calculated as I_{ox}/I_{red}. The TMD-CT contains 7 tryptophans and their side chain $^{1}H\varepsilon1$-$^{15}N\varepsilon1$ crosspeaks responded very differently to the addition of MTSL-labeled MA (Figure 2a). W678 and W680 near the N-terminal end of the TMD were not affected, as expected. Within the CT baseplate, 3 out of 5 tryptophans showed strong PRE and they are W757, W796, and W803, suggesting that interaction with MA is conformationally specific. Moreover, mapping residue-specific I_{ox}/I_{red} values to the TMD-CT NMR structure revealed two clusters of substantial PREs: 1) the inner cluster of residues 748−753 of the LLP2 and 2) the outer cluster of residues 802−806, 817, 819, 826, 837, 850−851, and 856 of LLP1 and LLP3 (Figure 2b).

We then used the intermolecular PREs to elucidate models of the complex between the NMR structure of the TMD-CT trimer and the crystal structure of the MA trimer to inform the functional mutagenesis. Due to limited PRE data obtainable for this system, the model construction assumed 1) the structures of the TMD-CT and MA trimers do not change significantly upon binding and 2) the 3-fold axes of the TMD-CT and MA align. The models were then generated by rotating the MA to achieve the best agreement with the measured PREs. Two models are tested here. Model 1 assumes a 1:1 stoichiometry of TMD-CT trimer to MA trimer and that the 3-fold axes of

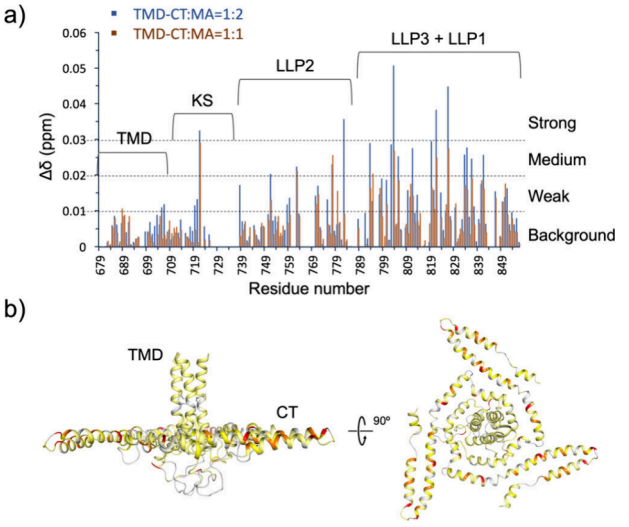

Figure 1. NMR evidence of a specific interaction between HIV-1 gp41 and MA. (a) CSP vs Residue number plot. CSP values are categorized as four different regions: background ($\Delta\delta < 0.012$; gray), low ($0.012 < \Delta\delta < 0.022$; yellow), medium ($0.022 < \Delta\delta < 0.032$; orange) and strong ($0.032 < \Delta\delta$, red). (b) Mapping of CSP values onto the TMD-CT structure with the color scheme defined in (a).

https://doi.org/10.1021/jacs.5c04597
J. Am. Chem. Soc. XXXX, XXX, XXX−XXX

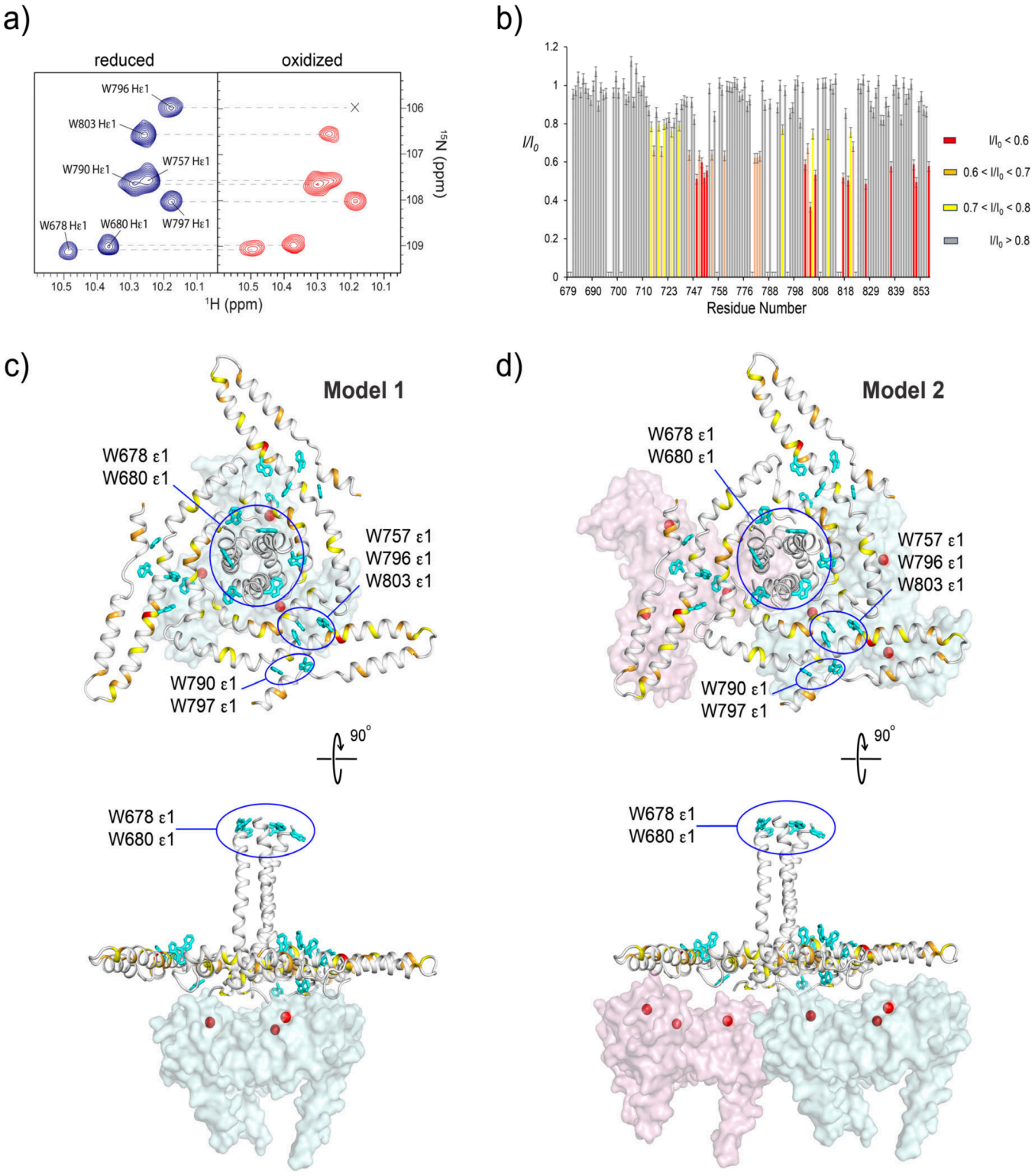

Figure 2. Measurement and analysis of intermolecular paramagnetic relaxation enhancement (PRE) between TMD-CT and MA. (a) Trp side chain $^{1}H\varepsilon1$-$^{15}N\varepsilon1$ crosspeaks from TROSY-HSQC spectrum of the TMD-CT in bicelles in the presence of reduced (left) and oxidized (right) MTSL-labeled MA. (b) PRE (I/I_0) vs Residue number plot. PRE values are categorized into four different regions: background ($I/I_0 > 0.8$; gray), low ($0.7 < I/I_0 < 0.8$; yellow), medium ($0.6 < I/I_0 < 0.7$; orange), and strong ($I/I_0 < 0.6$; red). (c) Mapping of intermolecular PREs onto the TMD-CT structure in Model 1 ([TMD-CT trimer]/[MA trimer] = 1). (d) PRE mapping as in (c) in Model 2 ([TMD-CT trimer]/[MA trimer] = 1/2). The red balls indicate the positions of the spin labels in the MA trimer.

the two trimers align (Figure 2c). Model 2 is based on a recent cryo-ET study of intact HIV virions suggesting that the Env is positioned between the two neighboring MA trimers of the underlying Gag-MA lattice;[35] in this model, one TMD-CT trimer is positioned against two MA trimers in the hexamer-of-trimer arrangement (Figure 2d). In Model 1, the spin label

https://doi.org/10.1021/jacs.5c04597
J. Am. Chem. Soc. XXXX, XXX, XXX−XXX

positions can explain the PREs in the core of the CT baseplate but not in the periphery, especially the significant PREs of residues 817, 819, and 826 on the far edge of the CT baseplate. Both types of PREs, however, could be explained by the interaction mode in Model 2. Interactions in both models are mediated primarily by electrostatic interactions between acidic residues of the CT baseplate and basic residues of the MA (Figure 3a).

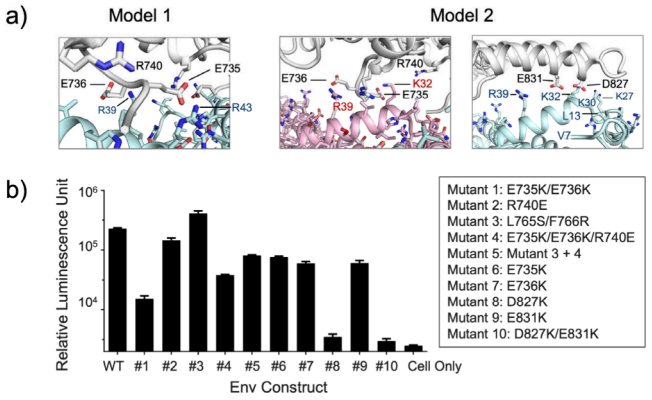

Figure 3. Functional mutagenesis of interaction between TMD-CT and MA. (a) Proposed acidic residues of TMD-CT (gray) for interacting with the MA basic residues (cyan or pink) in Model 1 and Model 2. (b) Viral infectivity (TCID50) of HIV-1 variants that contain mutation(s) in the CT designed to weaken the interaction according to interaction models 1 and 2 in (a). The R740E mutation was examined as a no-effect mutation.

Having the structural information, we next tested whether the weak but specific interaction between CT and MA observed in bicelles is relevant for viral assembly. We introduced 10 sets of mutations in the CT. These are 1) E735 K/E736 K, 2) R740E, 3) L765S/F766R, 4) E735 K/E736 K/R740E, 5) mutant 3 + 4, 6) E735 K, 7) E736 K, 8) D827 K, 9) E831 K, and 10) D827 K/E831 K. These Env mutants were tested for their effects on viral infectivity. Cell−cell fusion assay (Figure S3) and Western blots (Figure S4) were used for positive control and expression tests, respectively. The double mutant E735 K/E736 K showed a significant reduction (~60%) in viral infectivity (Figure 3b), consistent with both interaction models. However, neither single mutant R740E nor double mutant L765S/F766R exhibited significant effect on viral infectivity. The single mutant D827 K and the double mutant D827 K/E831 K showed a dramatic reduction (~80%) in viral infectivity (Figure 3b), consistent with Model 2.

In previous studies, Freed et al. performed comprehensive mutagenesis on the MA and found that many single MA mutations resulted in significantly reduced virus particle production.[27,28] While most of these mutations could disrupt MA folding according to the crystal structure, several mutations within the N-terminal fragment (residues 1−13) that are not important for folding also drastically reduced the assembly of infectious particles. For example, the L13E mutation blocks Env incorporation into the virions. According to Model 2, L13 is ~5 Å from D827 of the CT (Figure 3a). Mutating L13 to Glu is expected to introduce significant repulsion with D827 and thus disrupt the CT-MA interaction. In addition, the N-terminal loop also contains an Arg (R4) which is in the range for interacting with D827 and/or E831 but mutation of R4 has not been tested.

In conclusion, we have provided direct biochemical and structural evidence that the CT baseplate of HIV-1 gp41 formed in bicelles can specifically interact with MA in the homotrimeric form. PRE and mutagenesis data, however, suggest that the interaction does not align the 3-fold axis of the gp41 trimer with that of the MA trimer. We believe our finding explains the long-observed influence of gp41 CT mutations on viral assembly while providing preliminary structural information for guiding future studies to obtain complete visualization of the Env-MA organization on the viral membrane.

■ ASSOCIATED CONTENT

Supporting Information

The Supporting Information is available free of charge at https://pubs.acs.org/doi/10.1021/jacs.5c04597.

The SI includes Figures S1−S4 as well as description of all experiments and data analyses. (PDF)

■ AUTHOR INFORMATION

Corresponding Authors

Bing Chen − *Department of Pediatrics, Harvard Medical School, Boston, Massachusetts 02115, United States; Division of Molecular Medicine, Boston Children's Hospital, Boston, Massachusetts 02115, United States*; Email: bchen@crystal.harvard.edu

James J. Chou − *Department of Biological Chemistry and Molecular Pharmacology, Harvard Medical School, Boston, Massachusetts 02115, United States*; orcid.org/0000-0002-4442-0344; Email: james_chou@mail.sioc.ac.cn

Authors

Manish Chaubey − *Department of Biological Chemistry and Molecular Pharmacology, Harvard Medical School, Boston, Massachusetts 02115, United States*

Hailong Gao − *Department of Pediatrics, Harvard Medical School, Boston, Massachusetts 02115, United States; Division of Molecular Medicine, Boston Children's Hospital, Boston, Massachusetts 02115, United States*

Christy L. Lavine − *Center for Virology and Vaccine Research, Beth Israel Deaconess Medical Center, Boston, Massachusetts 02115, United States*

Michael S. Seaman − *Center for Virology and Vaccine Research, Beth Israel Deaconess Medical Center, Boston, Massachusetts 02115, United States*

Complete contact information is available at: https://pubs.acs.org/10.1021/jacs.5c04597

Author Contributions

#M.C. and H.G. contributed equally.

Notes

The authors declare no competing financial interest.

■ ACKNOWLEDGMENTS

This study was supported by NIH grant AI127193 to J.J.C. and B.C. NMR data were collected at the MIT-Harvard CMR (supported by NIH grants P41 GM132079 and S10 OD0253523-01A1).

REFERENCES

(1) Harrison, S. C. Viral membrane fusion. *Nature structural & molecular biology* **2008**, *15* (7), 690−698.

(2) Weissenhorn, W.; Dessen, A.; Harrison, S. C.; Skehel, J. J.; Wiley, D. C. Atomic structure of the ectodomain from HIV-1 gp41. *Nature* **1997**, *387*, 426−430.

(3) Chan, D. C.; Fass, D.; Berger, J. M.; Kim, P. S. Core structure of gp41 from the HIV envelope glycoprotein. *Cell* **1997**, *89*, 263−273.

(4) Julien, J. P.; Cupo, A.; Sok, D.; Stanfield, R. L.; Lyumkis, D.; Deller, M. C.; Klasse, P. J.; Burton, D. R.; Sanders, R. W.; Moore, J. P.; et al. Crystal structure of a soluble cleaved HIV-1 envelope trimer. *Science* **2013**, *342* (6165), 1477−1483.

(5) Fu, Q.; Shaik, M. M.; Cai, Y.; Ghantous, F.; Piai, A.; Peng, H.; Rits-Volloch, S.; Liu, Z.; Harrison, S. C.; Seaman, M. S.; et al. Structure of the membrane proximal external region of HIV-1 envelope glycoprotein. *Proc. Natl. Acad. Sci. U. S. A.* **2018**, *115* (38), E8892−E8899.

(6) Dev, J.; Park, D.; Fu, Q.; Chen, J.; Ha, H. J.; Ghantous, F.; Herrmann, T.; Chang, W.; Liu, Z.; Frey, G.; et al. Structural basis for membrane anchoring of HIV-1 envelope spike. *Science* **2016**, *353* (6295), 172−175.

(7) Piai, A.; Fu, Q.; Sharp, A. K.; Bighi, B.; Brown, A. M.; Chou, J. J. NMR Model of the Entire Membrane-Interacting Region of the HIV-1 Fusion Protein and Its Perturbation of Membrane Morphology. *J. Am. Chem. Soc.* **2021**, *143* (17), 6609−6615.

(8) Liu, J.; Bartesaghi, A.; Borgnia, M. J.; Sapiro, G.; Subramaniam, S. Molecular architecture of native HIV-1 gp120 trimers. *Nature* **2008**, *455* (7209), 109−113.

(9) Li, Z.; Li, W.; Lu, M.; Bess, J., Jr.; Chao, C. W.; Gorman, J.; Terry, D. S.; Zhang, B.; Zhou, T.; Blanchard, S. C.; et al. Subnanometer structures of HIV-1 envelope trimers on aldrithiol-2-inactivated virus particles. *Nat. Struct Mol. Biol.* **2020**, *27* (8), 726−734.

(10) Piai, A.; Fu, Q.; Cai, Y.; Ghantous, F.; Xiao, T.; Shaik, M. M.; Peng, H.; Rits-Volloch, S.; Chen, W.; Seaman, M. S.; et al. Structural basis of transmembrane coupling of the HIV-1 envelope glycoprotein. *Nat. Commun.* **2020**, *11* (1), 2317.

(11) Chen, J.; Kovacs, J. M.; Peng, H.; Rits-Volloch, S.; Lu, J.; Park, D.; Zablowsky, E.; Seaman, M. S.; Chen, B. HIV-1 ENVELOPE. Effect of the cytoplasmic domain on antigenic characteristics of HIV-1 envelope glycoprotein. *Science* **2015**, *349* (6244), 191−195.

(12) Shaik, M. M.; Peng, H.; Lu, J.; Rits-Volloch, S.; Xu, C.; Liao, M.; Chen, B. Structural basis of coreceptor recognition by HIV-1 envelope spike. *Nature* **2019**, *565* (7739), 318−323.

(13) Yang, Z.; Wang, H.; Liu, A. Z.; Gristick, H. B.; Bjorkman, P. J. Asymmetric opening of HIV-1 Env bound to CD4 and a coreceptor-mimicking antibody. *Nat. Struct Mol. Biol.* **2019**, *26* (12), 1167−1175.

(14) Kwong, P. D.; Wyatt, R.; Robinson, J.; Sweet, R. W.; Sodroski, J.; Hendrickson, W. A. Structure of an HIV gp120 envelope glycoprotein in complex with the CD4 receptor and a neutralizing human antibody. *Nature* **1998**, *393* (6686), 648−659.

(15) Lyumkis, D.; Julien, J. P.; de Val, N.; Cupo, A.; Potter, C. S.; Klasse, P. J.; Burton, D. R.; Sanders, R. W.; Moore, J. P.; Carragher, B.; et al. Cryo-EM structure of a fully glycosylated soluble cleaved HIV-1 envelope trimer. *Science* **2013**, *342* (6165), 1484−1490.

(16) Pancera, M.; Zhou, T.; Druz, A.; Georgiev, I. S.; Soto, C.; Gorman, J.; Huang, J.; Acharya, P.; Chuang, G. Y.; Ofek, G.; et al. Structure and immune recognition of trimeric pre-fusion HIV-1 Env. *Nature* **2014**, *514* (7523), 455−461.

(17) Hill, C. P.; Worthylake, D.; Bancroft, D. P.; Christensen, A. M.; Sundquist, W. I. Crystal structures of the trimeric human immunodeficiency virus type 1 matrix protein: implications for membrane association and assembly. *Proc. Natl. Acad. Sci. U. S. A.* **1996**, *93* (7), 3099−3104.

(18) Freed, E. O.; Englund, G.; Martin, M. A. Role of the basic domain of human immunodeficiency virus type 1 matrix in macrophage infection. *J. Virol* **1995**, *69* (6), 3949−3954.

(19) Ono, A.; Ablan, S. D.; Lockett, S. J.; Nagashima, K.; Freed, E. O. Phosphatidylinositol (4,5) bisphosphate regulates HIV-1 Gag targeting to the plasma membrane. *Proc. Natl. Acad. Sci. U. S. A.* **2004**, *101* (41), 14889−14894.

(20) Chukkapalli, V.; Ono, A. Molecular determinants that regulate plasma membrane association of HIV-1 Gag. *J. Mol. Biol.* **2011**, *410* (4), 512−524.

(21) Sundquist, W. I.; Kräusslich, H. G. HIV-1 assembly, budding, and maturation. *Cold Spring Harb Perspect Med.* **2012**, *2* (7), No. a006924.

(22) Zhu, P.; Liu, J.; Bess, J., Jr.; Chertova, E.; Lifson, J. D.; Grisé, H.; Ofek, G. A.; Taylor, K. A.; Roux, K. H. Distribution and three-dimensional structure of AIDS virus envelope spikes. *Nature* **2006**, *441* (7095), 847−852.

(23) Checkley, M. A.; Luttge, B. G.; Freed, E. O. HIV-1 envelope glycoprotein biosynthesis, trafficking, and incorporation. *J. Mol. Biol.* **2011**, *410* (4), 582−608.

(24) Nguyen, D. H.; Hildreth, J. E. Evidence for budding of human immunodeficiency virus type 1 selectively from glycolipid-enriched membrane lipid rafts. *J. Virol* **2000**, *74* (7), 3264−3272.

(25) Ono, A.; Freed, E. O. Plasma membrane rafts play a critical role in HIV-1 assembly and release. *Proc. Natl. Acad. Sci. U. S. A.* **2001**, *98* (24), 13925−13930.

(26) Rousso, I.; Mixon, M. B.; Chen, B. K.; Kim, P. S. Palmitoylation of the HIV-1 envelope glycoprotein is critical for viral infectivity. *Proc. Natl. Acad. Sci. U. S. A.* **2000**, *97* (25), 13523−13525.

(27) Freed, E. O.; Orenstein, J. M.; Buckler-White, A. J.; Martin, M. A. Single amino acid changes in the human immunodeficiency virus type 1 matrix protein block virus particle production. *J. Virol* **1994**, *68* (8), 5311−5320.

(28) Freed, E. O.; Martin, M. A. Domains of the human immunodeficiency virus type 1 matrix and gp41 cytoplasmic tail required for envelope incorporation into virions. *J. Virol* **1996**, *70* (1), 341−351.

(29) Murakami, T.; Freed, E. O. Genetic evidence for an interaction between human immunodeficiency virus type 1 matrix and alpha-helix 2 of the gp41 cytoplasmic tail. *J. Virol* **2000**, *74* (8), 3548−3554.

(30) Vincent, M. J.; Melsen, L. R.; Martin, A. S.; Compans, R. W. Intracellular interaction of simian immunodeficiency virus Gag and Env proteins. *J. Virol* **1999**, *73* (10), 8138−8144.

(31) Cosson, P. Direct interaction between the envelope and matrix proteins of HIV-1. *EMBO journal* **1996**, *15* (21), 5783−5788.

(32) Manrique, J. M.; Affranchino, J. L.; González, S. A. In vitro binding of simian immunodeficiency virus matrix protein to the cytoplasmic domain of the envelope glycoprotein. *Virology* **2008**, *374* (2), 273−279.

(33) Murakami, T.; Freed, E. O. The long cytoplasmic tail of gp41 is required in a cell type-dependent manner for HIV-1 envelope glycoprotein incorporation into virions. *Proc. Natl. Acad. Sci. U. S. A.* **2000**, *97* (1), 343−348.

(34) Tan, A.; Pak, A. J.; Morado, D. R.; Voth, G. A.; Briggs, J. A. G. Immature HIV-1 assembles from Gag dimers leaving partial hexamers at lattice edges as potential substrates for proteolytic maturation. *Proc. Natl. Acad. Sci. U. S. A.* **2021**, *118* (3), No. e2020054118.

(35) Mangala Prasad, V.; Leaman, D. P.; Lovendahl, K. N.; Croft, J. T.; Benhaim, M. A.; Hodge, E. A.; Zwick, M. B.; Lee, K. K. Cryo-ET of Env on intact HIV virions reveals structural variation and positioning on the Gag lattice. *Cell* **2022**, *185* (4), 641−653.e617.

https://doi.org/10.1021/jacs.5c04597
J. Am. Chem. Soc. XXXX, XXX, XXX−XXX